Lanthanide−Group 12 Metal Chalcogenolates: A Versatile Class of Compounds

M. Berardini, T. J. Emge, and J. G. Brennan*

Department of Chemistry, Rutgers, The State University of New Jersey, Piscataway, New Jersey 08855-0939

Received June 8, 1995[⊗]

Heterometallic chalcogenolate compounds containing both lanthanide (Ln) and group 12 metals (M) represent an extremely broad molecular class, having the general formula $LnM(EPh)_x(L)_y$, where L is a neutral donor ligand. In this paper we show how M, L, and the ratio Ln:M can be varied to give bi-, tetra-, penta-, and hexametallic chalcogenolates. The compounds $[(py)_3Eu(\mu_2\text{-}SePh)_2(\mu_3\text{-}SePh)Hg(SePh)]_2$ (**1**), $(THF)_4Eu(\mu_2\text{-}SePh)_3ZnSePh$ (**2**), $[Sm(THF)_7][Zn_4(\mu_2\text{-}SePh)_6(SePh)_4]$ (**3**), and $[Yb(THF)_6][Hg_5(\mu_2\text{-}SePh)_8(SePh)_4]\cdot 2THF$ (**4**) have been prepared, and their structures have been established by low temperature single crystal X-ray diffraction. The synthesis and structural characterization of the heterometallic chalcogenolate $[(py)_2Sm(SePh)(\mu\text{-}SePh)_3Na(py)_2]_2$ (**5**) is also described in order to compare the relative effects of the alkali and group 12 metals on heterometallic structure and electronic properties. From the crystal structures it is clear that the group 12 ion polarizes Se electron density away from the Ln ion, weakening the Ln−Se bond, and increasing the Ln−Se bond length. UV−visible data support the structural interpretations, with Ln(II) metal-to-pyridine charge transfer and lanthanide(III) selenolate to metal charge transfer absorption energies, both indicating that the group 12 metal withdraws electron density from the lanthanide ion. Unambiguous assignment of heterometallic solution structure is impossible, because the molecules are fluctional, and the solution structure is solvent dependent. However, from spectroscopic measurements, and from the isolation of **1** in 90% yield, it is clear that the compounds do maintain some form of heterometallic structure in donor solvents as basic as pyridine. Crystal data (**1**−**3** and **5**, Mo Kα; **4**, Cu Kα; −80 to −100 °C): **1**, space group $P\bar{1}$, a = 12.374(4) Å, b = 13.381(3) Å, c = 14.222(4) Å, α = 62.36(3)°, β = 70.96(3)°, γ = 70.14(2)°, V = 1921Å, Z = 2; **2**, space group P_n, a = 10.991(4) Å, b = 20.051(3) Å, c = 19.522(4) Å, β = 99.75(3)°, V = 4240 Å, Z = 4; **3**, triclinic space group $P\bar{1}$, a = 14.268(6) Å, b = 19.220(10) Å, c = 19.539(4) Å, α = 92.64(3), β = 104.20(3)°; γ = 109.32(4)°, V = 4854 Å, Z = 2; **4**, monoclinic space group $P2_1/c$, a = 14.239(3) Å, b = 48.846(6) Å, c = 17.282(4) Å, β = 113.79(2)°, V = 10999 Å, Z = 4; **5**, monoclinic space group $C2/c$, a = 23.822(5) Å, b = 16.902(2) Å, c = 21.388(3) Å, β = 93.35(2)°, V = 8597 Å, Z = 8.

Introduction

The coordination chemistry of lanthanide (Ln) ions bound to anionic thiolate, selenolate, or tellurolate (chalcogenolate) ligands is a rapidly developing area of research that addresses questions related to the fundamental nature of the lanthanide chalcogen bond. While bonding in solid state lanthanide chalcogenide compounds has long been discussed in terms of covalent bonding character,[1] in molecular systems the interaction between these hard, ionic Lewis acids and the soft, covalent chalcogenolate anions has not been fully examined, and little is known about the relative factors that contribute to the stability of molecular Ln−chalcogen bonds. Sterically demanding, highly electronegative pentamethylcyclopentadienyl[2] (Cp*) and heteroallylic[3] ligands were used to facilitate the first isolation and structural characterization of lanthanide complexes containing direct bonds to the less electronegative chalcogens Se and Te (as well as numerous Ln−S bonds), at a time when homoleptic chalcogenolates were thought to be insoluble materials.[4] Unfortunately, the interpretations of bond geometries in the Cp* and heteroallylic complexes were complicated by significant ligand−ligand repulsive interactions. In the past few years a number of research groups have found that large, electronegative ancillary ligands are not a prerequisite for isolating stable complexes with Ln−chalcogen bonds, and there

[⊗] Abstract published in *Advance ACS Abstracts,* October 1, 1995.

(1) (a) Gerth, G.; Kienle, P.; Luchner, K. *Phys. Lett. A* **1968**, *27*, 557−8. (b) Eatough, N. L.; Hall, H. T. *Inorg. Chem.* **1970**, *9*, 417−8. (c) Dagys, R. S.; Anisimov, F. G. *Sov. Phys. Solid State* **1984**, *26*, 547−8 . (d) Wachter, P. *Crit. Rev. Solid State* **1972**, *3*, 189- 241. (e) Byrom, E.; Ellis, D. E.; Freeman, A. J. *Phys. Rev. B* **1976**, *14*, 3558−68. (f) Zhukov, V. P.; Gubanov, V. A.; Weber, J. *J. Chem. Phys. Solids* **1981**, *42*, 631−9.

(2) (a) Schumann, H.; Albrecht, I.; Hahn, E. *Angew. Chem. Int. Ed. Engl.* **1985**, *24*, 985−6. (b) Berg, D.; Burns, C.; Andersen, R. A.; Zalkin, A. *Organometallics* **1988**, *8*, 1858−63. (c) Berg, D. J.; Burns, C.; Andersen, R. A.; Zalkin, A. *Organometallics* **1989**, *8*, 1865−70. (d) Zalkin, A.; Berg, D. J. *Acta Crystallogr.* **1988**, *44C*, 1488−1489. (e) Evans, W.; Grate, J. W.; Bloom, I.; Hunter, W. E.; Atwood, J. L. *J. Am. Chem. Soc.* **1985**, *107*, 405−9. (f) Evans, W; Rabe, G.; Ziller, J.; Doedens, R. *Inorg. Chem.* **1994**, *33*, 2719−26.

(3) Welder, M.; Noltemeyer, M.; Pieper, U.; Schmidt, H.; Stalke, D.; Edelmann, F. *Angew. Chem., Int. Ed. Engl.* **1990**, *29*, 894−6.

(4) Gharia, K. S.; Singh, M.; Mathur, S.; Roy, R.; Sankhla, B. S. *Synth. React. Inorg. Met.-Org. Chem.* **1982**, *12*, 337−345.

(5) (a) Strzelecki, A. R.; Timinski, P. A.; Hesel, B. A.; Bianconi, P. A. *J. Am. Chem. Soc.* **1992**, *114*, 3159−3160. (b) Cary, D. R.; Arnold, J. *J. Am. Chem. Soc.* **1993**, *115* , 2520−2521. (c) Berardini, M.; Emge, T.; Brennan, J. G. *J. Chem. Soc., Chem. Commun.* **1993**, 1537−8. (d) Berardini, M.; Emge, T.; Brennan, J. G. *J. Am. Chem. Soc.* **1993**, *115*, 8501−2. (e) Khasnis, D. V.; Lee, J.; Brewer, M.; Emge, T. J.; Brennan, J. G. *J. Am. Chem. Soc.* **1994**, *116*, 7129−33. (f) Brewer, M.; Khasnis, D.; Buretea, M.; Berardini, M.; Emge, T. J.; Brennan, J. G. *Inorg. Chem.* **1994**, *33*, 2743−7 (g) Carey, D. R. Arnold, J. *Inorg. Chem.* **1994**, *33*, 1791−5. (h) Mashima, K.; Nakayama, Y.; Kanehisa, N.; Kai, Y.; Nakamura, A. *J. Chem. Soc. Chem. Commun.* **1993**, 1847−8. (i) Strzelecki, A. R.; Likar, C.; Hesel, B. A.; Utz, T.; Lin, M. C.; Bianconi, P. A. *Inorg. Chem.* **1994**, *33*, 5188−94. (j) Mashima, K.; Nakayama, Y.; Fukumoto, H.; Kanehisa, N.; Kai, Y.; Nakamura, A. *J. Chem. Soc., Chem. Commun.* **1994**, 2523−4. (k) Tatsumi, K.; Amemiya, T.; Kawaguchi, H.; Tani, K. *J. Chem. Soc., Chem. Commun.* **1993**, 773−4. (l) Cetinkaya, B.; Hitchcock, P. B.; Lappert, M. F.; Smith, R. G. *J. Chem. Soc. Chem. Commun.* **1992**, 932−3. (m) Lee, Jongseong, Brewer, M.; Berardini, M.; Brennan, J. *Inorg. Chem.* **1995**, *34*, 3215. (n) Berardini, M.; Brennan, J. *Inorg. Chem.*, in press.

0020-1669/95/1334-5327$09.00/0

are now a number of reports describing the synthesis and characterization of lanthanide complexes with chalcogenolates as the *only* anions.[5] In addition to the fundamental importance of these compounds, Ln chalcogenolates have a number of potential applications as Ln doping sources in S-, Se-, or Te-based semiconductor[6] and fiber optic technologies.[7]

Recently, the syntheses and structural characterization of the first heterometallic Ln−group 12 metal chalcogenolates were reported. Both $Eu(SePh)_2$ and $Sm(SePh)_3$ were shown to react with $Hg(SePh)_2$ to form the tetrametallic selenolate clusters $[(THF)_3Eu(SePh)_2Hg(SePh)_2]_2$ and $[(THF)_2Sm(SePh)_2Hg(SePh)_2]_2$.[8] These heterometallic compounds are simple, readily prepared, and sterically uncongested derivatives of lanthanide chalcogenolates, and, as such, can serve to enhance our understanding of Ln−chalcogen bonding and lanthanide chalcogenolate reactivity. In this paper the broad scope of heterometallic chalcogenolate chemistry is established with examples of how neutral donor, group 12 metal, and Ln:group 12 metal ratios can be systematically varied to give bi-, tetra-, penta-, and hexametallic benzeneselenolate compounds. The effects of these synthetic manipulations on the structural and electronic properties of the heterometallic complexes are described, and the variety of structures are rationalized in terms of the bonding character of the component metal ions. Solvent effects are shown to play a significant role in determining heterometallic structure.

Experimental Section

General Data. All syntheses were carried out under ultrapure nitrogen (JWS), using conventional drybox or Schlenk techniques. Solvents (Fisher) were refluxed over molten alkali metals (diethyl ether, THF, pyridine) or P_2O_5 (CH_3CN), and collected immediately prior to use. PhSeSePh was purchased from either Aldrich or Strem, and recrystallized from hexane. Eu, Sm, Yb, Zn, and Hg were purchased from Strem. Melting points were taken in sealed capillaries and are uncorrected. IR spectra were taken on a Mattus Cygnus 100 FTIR spectrometer and recorded from 4000−450 cm^{-1}, as a Nujol mull. Electronic spectra were recorded on a Varian DMS 100S spectrometer with the samples in a 0.10 mm quartz cell attached to a teflon stopcock. Elemental analyses were preformed by Quantitative Technologies, Inc. (Salem, NJ). NMR spectra were obtained on either a Varian Gemini 200 MHz or Varian 400 MHz NMR spectrometer and are reported in δ (ppm).

$[(py)_3Eu(\mu_2\text{-}SePh)_2(\mu_3\text{-}SePh)Hg(SePh)]_2$ (1). Hg (3.1 g, 15.4 mmol), Eu (0.6 g, 3.9 mmol), and diphenyl diselenide (2.5 g, 7.9 mmol) were added to pyridine (20 mL) while the mixture was stirred, and an orange solution developed within hours. After 2 days, the bright orange solution was filtered and layered with diethyl ether (50 mL) to give yellow crystals of **1** (3.28 g, 90%; mp 150 °C dec (turned green 227−230 °C)). The molecule crystallized with a pyridine solvent molecule, but this pyridine appeared to diffuse from the lattice within an hour of isolation. Anal. Calcd for $EuHgC_{39}H_{35}N_3Se_4$: C, 38.6; H: 2.91; N, 3.46. Found: C, 38.1; H, 2.91; N, 3.34. IR: 2900 (s), 2724 (w), 2671 (w), 1592 (w), 1569 (w), 1461 (s), 1377 (s), 1303 (w), 1152 (w), 1062 (w), 998 (w), 727 (m), 701 (w), 614 (w), 464 (w) cm^{-1}. The ^1H NMR (CD_3CN) spectrum contained broad peaks at 8.2 (1H), 7.8(2H), and 6.6(2H) due to the pyridine ligands, and significantly sharper resonances at 7.56(2 H), 7.06-(3 H) due to the benzeneselenolate ligands. λ_{max}: 380 nm (in pyridine).

$(THF)_4Eu(\mu_2\text{-}SePh)_3ZnSePh$ (2). $[(THF)_3Eu(\mu\text{-}SePh)_3Hg(SePh)]_2$ (0.6 g, 0.5 mmol) was dissolved in THF (30 mL), and Zn (33 mg, 0.50 mmol) was added to the solution. After 5 days, the yellow solution was filtered to remove mercury, and the filtrate was concentrated to 25 mL. When the filtrate was allowed to stand at room temperature, pale yellow crystals (0.45 g, 80%) precipitated from solution. These crystals turned opaque above 100 °C, dark yellow above 170 °C, and dark red by 330 °C, but they did not appear to melt. Once isolated, the compound desolvated within an hour to a stoichiometry of 3:1 THF:Eu. Anal. Calcd for $EuZnC_{36}H_{44}O_3Se_4$: C, 40.9; H, 4.20. Found: C, 40.7; H, 4.35. IR: 2900 (s), 2724 (w), 2671 (w), 1571 (w), 1461 (s), 1377 (s), 1305 (w), 1262 (w), 1154 (w), 1068 (w), 1021 (w), 871 (w), 732 (m), 691 (w), 664 (w), 463 (w) cm^{-1}. The ^1H NMR spectrum (CD_3CN) contained very broad peaks at 8.45 ($w_{1/2}$ = 170 Hz), 7.60 ($w_{1/2}$ = 50 Hz), 7.10 ($w_{1/2}$ = 50 Hz), and 6.31 ($w_{1/2}$ = 230 Hz)ppm, and THF resonances at 3.64 ($w_{1/2}$ = 60 Hz) and 1.75 ($w_{1/2}$ = 20 Hz) ppm, that were too broad for accurate integration. λ_{max}: 352 nm (in pyridine).

$[Sm(THF)_7][Zn_4(\mu_2\text{-}SePh)_6(SePh)_4]$ (3). Method a. A mixture of Sm (0.28 g, 1.5 mmol), diphenyl diselenide (2.34 g, 7.5 mmol), Zn metal (0.39 g, 6.0 mmol), and Hg (84 mg, 0.42 mmol) in THF (100 mL) was refluxed for 18 h. The green solution was filtered and cooled to room temperature, and a purple oil formed immediately. After 1 day, purple crystals of **3** (2.3 g, 62%; mp 56−60 °C) were isolated. Anal. Calcd for $SmZn_4C_{88}H_{106}O_7Se_{10}$: C, 42.7; H, 4.32. Found: C, 42.2; H, 4.26. IR: 2900 (s), 2671 (w), 2724 (w), 1570 (w), 1461 (s), 1377 (s), 1295 (w), 1264 (w), 1173 (w), 1066 (m), 1015 (m), 914 (w), 857 (m), 730 (m), 914 (m), 688 (m), 664 (m), 464 (m) cm^{-1}. The ^1H NMR spectrum (CD_3CN) contained broad overlapping multiplets at 7.48, 6.95, and 6.82 ppm (50 H) and THF resonances at 3.57 (m, 28 H, $w_{1/2}$ = 15 Hz), 1.71 (m, 28 H, $w_{1/2}$ = 15 Hz). λ_{max}: 567 nm (THF). λ_{max}: 610 nm (1:10 PEt_3:THF). λ_{max}: 676 nm (CH_3CN).

Method b. $[(THF)_2Sm(SePh)_3Hg(SePh)_2]_2$[8] (3.0 g, 2.35 mmol) and Zn metal (0.40 g, 6.1 mmol) were added to THF (100 mL), and the solution was stirred continuously. After 3 days at room temperature the solution was refluxed for 30 min,

(6) (a) Pomrenke, G. S.; Klein, P. B.; Langer, D. W. *Rare Earth Doped Semiconductors*; MRS Symposium 301: Materials Research Society: Pittsburgh, PA, 1993. (b) Singer, K. E.; Rutter, P.; Praker, A. R.; Wright, A. C. *Appl. Phys. Lett.* **1994**, *64*, 707−9. (c) Swiatek, K.; Godlewski, M.; Niinisto, L.; Leskela, M. *J. Appl. Phys.* **1993**, *74*, 3442−6. (d) Taniguchi, M.; Takahei, K. *J. Appl. Phys* **1993**, *73*, 943−7. (e) Jourdan, N.; Yamaguchi, H.; Harikoshi, Y. *Jpn. J. Appl. Phys.* **1993**, *32*, 1784−7. (f) Kalboussi, A.; Moneger, S.; Marrakchi, G.; Guillot, G.; Lambert, B.; Guivarc'h, A. *J. Appl. Phys.* **1994**, *75*, 4171−5. (g) Takahei, K.; Taguchi, A.; Harikoshi, Y.; Nakata, J. *J. Appl. Phys.* **1994**, *76*, 4332−9. (h) Lozykowski, H. J.; Alshawa, A. K.; Brown, I. *J. Appl. Phys.* **1994**, *76*, 4836−46. (i) Kimura, T.; Isshiki, H.; Ishida, H.; Yugo, S.; Saito, R.; Ikoma, T. *J. Appl. Phys.* **1994**, *76*, 3714−9. (j) Charreire, Y.; Tolomen-Kivimaki, O.; Leskela, M.; Cortes, R.; Nykanen, E.; Soininen, P.; Niinisto, L. *Program and Abstracts of the ICFE-2, Aug. 1−6, 1994*, Kansikas, J., Leslela, M., Eds.; University of Helsinki, Helsinki, Finland, 1994; p 326. (k) Charreire, Y.; Marbeuf, A.; Tourillon, G.; Leskela, M.; Niinisto, L.; Nykanen, E.; Soininen, P.; Tolonen, O. *J. Electrochem. Soc.* **1992**, *139*, 619−21. (l) Charreire, Y.; Svoronos, D. R.; Ascone, I.; Tolonen, O.; Niinisto, L.; Leskela, M. *J. Electrochem. Soc.* **1993**, *140*, 2015−9.

(7) (a) Kanamori, T.; Terunuma, Y.; Takahashi, S.; Miyashita, T. *J. Lightwave Tech.* **1984**, *LT2*, 607. (b) Kumta, P. N.; Risbud, S. H. *Ceram. Bull.* **1990**, *69*, 1977. (c) Nishii, J.; Morimoto, S.; Yokota, R.; Yamagishi, T. *J. Non-Cryst. Solids* **1987**, *95/96*, 641−6. (d) Savage, J. A. *Infrared Optical Materials and Their Antireflection Coatings*; Adam Hilger Ltd: Bristol, U.K., 1985; pp 79−94. (e) Nishii, J.; Morimoto, S.; Inagawa, I.; Iizuka, R.; Yamashita, T.; Yokota, R.; Yamagishi, T. *J. Non-Cryst. Solids* **1992**, *140*, 199−208. (f) Sanghara, J. S.; Busse, L. E.; Aggarwall, I. D. *J. Appl. Phys.* **1994**, *75*, 4885−91. (g) Katsugama, T.; Matsumura, H. *J. Appl. Phys.* **1994**, *75*, 2743−8.

(8) Berardini, M.; Emge, T. J.; Brennan, J. G. *J. Am. Chem. Soc.* **1994**, *116*, 6941−2.

Table 1. Summary of Crystallographic Details for **1–5**

	1	2	3	4	5
space group	$P\bar{1}$	P_n	$P\bar{1}$	$P2_1/c$	$C2/c$
a (Å)	12.374(4)	10.991(4)	14.268(6)	14.239(3)	23.822(5)
b (Å)	13.381(3)	20.051(3)	19.220(10)	48.486(6)	16.902(2)
c (Å)	14.222(4)	19.522(4)	19.539(4)	17.282(4)	21.388(3)
α (deg)	62.36(3)	90	92.64(3)	90	90
β (deg)	70.96(3)	99.75(3)	104.20(3)	113.79(2)	93.35(2)
γ (deg)	70.14(2)	90	109.32(4)	90	90
V (Å^3)	1921.4(9)	4240(2)	4854(3)	10999(4)	8597(2)
Z	2	4	2	4	8
r_{calc} (Mg/m^{-3})	2.098	1.770	1.744	2.189	1.721
no. of nique reflns [$I > 2\sigma(I)$]	5320	5351	5136	7509	3780
$R(F)$	0.042	0.054	0.077	0.150	0.055
$R_w(F^2)$	0.094	0.107	0.177	0.387	0.128

[a] Definitions: $R(F_o) = \sum||F_o| - |F_c||/\sum|F_o|$; $R_w(F_o^2) = \{\sum[w(F_o^2 - F_c^2)^2]/\sum[w(F_o^2)^2]\}^{1/2}$. Additional crystallographic details are given in the Supporting Information.

filtered, and cooled to room temperature. The oil which deposited on cooling slowly formed **3** (1.5 g, 70%) as purple crystals.

[Yb(THF)$_6$][Hg$_5$(μ_2-SePh)$_8$(SePh)$_4$]·2THF (4). Yb (0.52 g, 3.0 mmol), diphenyl diselenide (4.7 g, 15 mmol), and Hg (9.8 g, 49 mmol) were suspended in THF (30 mL), and the mixture was stirred continuously. After a day the resultant yellow solution was filtered and layered with diethyl ether (70 mL). An orange oil formed within 24 h. After a week the mixture was brought to dryness, redissolved in THF (10 mL), and cooled to 0 °C, upon which a large amount of yellow solid formed. THF (30 mL) was added, and the solid was redissolved by heating the solution to 60 °C. Cooling to room temperature gave large yellow blocks—a second crop of crystals was obtained by decanting the filtrate, reducing the volume by 50%, and cooling to 0 °C. Total yield: 8.0 g, 92%; mp 60 −64 °C. The compound crystallized with two THF molecules which were detected by NMR when the sample was prepared within a few seconds of compound isolation. The compound was extremely prone to THF desolvation—the yellow crystals became opaque within minutes of isolation. Elemental analysis indicated that THF loss was complete within an hour. Anal. Calcd for $YbHg_5C_{72}H_{60}Se_{12}$: C, 27.8; H, 2.44. Found: C, 28.3; H, 1.99. IR: 2900 (s), 2734 (w), 2671 (w), 1570 (w), 1461 (s), 1377 (s), 1295 (w), 1264 (w), 1173 (w), 1066 (m), 1015 (m), 914 (w), 856 (w), 730 (m), 688 (w), 664 (w), 464 (m) cm^{-1}. ^{1}H NMR (CD_3CN, 20 °C): 7.48 (d, 15H), 7.03 (m, 30 H), 3.77 (m, 24H), 1.85 (m, 24H). λ_{max}: 372 nm (THF). The compound was unstable in acetonitrile; attempts to obtain a ^{13}C NMR spectrum in CD_3CN led to the precipitation of crystalline Hg(SePh)$_2$ (**6**). In an attempt to quantify the amount of precipitating **6**, **4** (1.3 g, 0.39 mmol) was dissolved in acetonitrile (15 mL) and the solution was layered with diethyl ether (30 mL). Within a few hours yellow plates began to crystallize. After 2 days the solution was decanted to give air stable yellow crystals (0.10 g, 10%) that were identified as Hg(SePh)$_2$ by melting point, ^{1}H NMR spectroscopy, and single crystal X-ray diffraction. The compound reacted with pyridine to form a trivalent ytterbium complex—addition of pyridine (5 mL) to **4** (1.3 g) resulted in the precipitation of elemental Hg which was identified visually. ^{1}H NMR (NC_5D_5, 20 °C): broad peaks ($w_{1/2}$ ca. 100 Hz) at 8.55, 7.41, and 7.03 (due to rapidly exchanging free and coordinated pyridine), 7.67 (15 H, $w_{1/2}$ = 90 Hz) and 7.04 (30 H, $w_{1/2}$ = 97 Hz) (benzeneselenolate) ppm, and 3.58 (m, 24H, $w_{1/2}$ = 13 Hz) and 1.58 (24 H, $w_{1/2}$ = 13 Hz) (THF) ppm. The optical spectrum was concentration dependent in pyridine. λ_{max}: 414 nm (1.9×10^{-3} M). λ_{max}: 388, 440 nm (7.5×10^{-2} M).

[(py)$_2$Sm(SePh)(μ-SePh)$_3$Na(py)$_2$]$_2$ (5). Diphenyl diselenide (0.47 g, 1.5 mmol) was dissolved in diethyl ether (30 mL), and Na[HBEt$_3$] (3.0 mL of a 1.0 M solution in THF, 3.0 mmol) was added *via* syringe. The solution was stirred for 20 min, and the solvent was removed under vacuum, to give a white solid. Diphenyl diselenide (1.4 g, 4.5 mmol), Hg (0.1 g, 0.5 mmol), Sm (0.45g, 3.0 mmol), and THF (60 mL) were added to the NaSePh, and the mixture was stirred for 24 h. The deep orange solution was filtered, concentrated (25–30 mL), and layered with diethyl ether (70 mL). After 1 week a small amount of white solid had formed. The Schlenk tube was agitated to completely mix the THF and ether, and the solution was filtered and cooled (−20 °C). The resultant orange oil crystallized over a period of 2 months. The solution was decanted to yield crystals of **5** (1.5 g, 45%; the compound did not melt but lost pyridine above 70 °C and turned deep red by 130 °C). Anal. Calcd for $SmNaC_{44}H_{40}N_4Se_4$: C, 47.4; H, 3.63; N, 5.03. Found: C, 46.4; H, 3.42; N, 4.86. IR: 2926 (s), 2855 (s), 1598 (w), 1572 (w), 1465 (s), 1378 (m), 1260 (w), 1218 (w), 1146 (w), 1068 (w), 1020 (w), 801 (w), 732 (m), 690 (m), 624 (w), 467 (w) cm^{-1}. ^{1}H NMR (C_5D_5N, 20 °C) 8.56 (2H, m), 7.72 (1H, t), 7.29 (4H, m), 6.72 (3H, m) ppm. λ_{max}: 305, 314 nm (pyridine).

X-ray Structure Determination of 1–5. Data for **1–5** were collected on a CAD4 diffractometer with graphite monochromatized Mo Kα radiation, λ = 0.710 73 Å (except for **4**, where Cu Kα, λ = 1.5418Å was used) at low temperatures (−80 to −120 °C). In all structures, three check reflections were measured every hour and showed no significant intensity variation. The data were corrected for Lorenz effects and polarization. The absorption corrections were based on a Gaussian grid method (SHELX76).[9] The structures were solved by Patterson and direct methods (SHELXS86).[10] All non-hydrogen atoms were refined (SHELXL93)[11] based upon F_{obs}^2. All hydrogen atom coordinates were calculated with idealized geometries (SHELXL93). Crystallographic data and final R indices are given in Table 1. Complete crystallographic details are given in the Supporting Information. The following restraints were used in the refinements (SHEXL93).

(**1**) All C and N atoms were restrained with esd 0.01 so that their U_{ij} components approximated isotropic behavior; all C or N atoms closer than 1.7 Å to each other were restrained with esd of 0.02 to have the same U_{ij} components.

(9) Sheldrick, G. M. SHELX76, Program for Crystal Structure Determination. Univ. of Cambridge, England, 1976.
(10) Sheldrick, G. M. SHELXS86, Program for the Solution of Crystal Structures. University of Gottingen, Germany, 1986.
(11) Sheldrick, G. M. SHELXL93, Program for Crystal Structure Refinement. University of Gottingen, Germany, 1993.

Table 2. Significant Bond Lengths (Å) and Angles (deg) for **1**[a]

Hg−Se(3)	2.545(1)	Hg−Se(2)	2.665(1)
Hg−Se(4)	2.688(1)	Hg−Se(1)	2.787(1)
Eu−N(3)	2.659(7)	Eu−N(1)	2.671(7)
Eu−N(2)	2.688(7)	Eu−Se(1)′	3.131(1)
Eu−Se(2)	3.146(1)	Eu−Se(4)′	3.153(1)
Eu−Se(1)	3.184(1)	Se(1)−C(1)	1.920(8)
Se(2)−C(7)	1.919(8)	Se(3)−C(13)	1.911(7)
Se(4)−C(19)	1.929(8)		
Se(3)−Hg−Se(2)	122.72(4)	Se(3)−Hg−Se(4)	124.89(4)
Se(2)−Hg−Se(4)	98.59(4)	Se(3)−Hg−Se(1)	108.90(4)
Se(2)−Hg−Se(1)	96.16(4)	Se(4)−Hg−Se(1)	100.01(4)
N(3)−Eu−N(1)	149.2(2)	N(3)−Eu−N(2)	72.6(2)
N(1)−Eu−N(2)	77.8(2)	N(3)−Eu−Se(1)′	135.4(1)
N(1)−Eu−Se(1)′	75.4(2)	N(2)−Eu−Se(1)′	150.0(2)
N(3)−Eu−Se(2)	102.5(2)	N(1)−Eu−Se(2)	87.5(2)
N(2)−Eu−Se(2)	94.0(2)	Se(1)′−Eu−Se(2)	71.78(4)
N(3)−Eu−Se(4)′	88.4(2)	N(1)−Eu−Se(4)′	95.2(2)
N(2)−Eu−Se(4)′	112.0(2)	Se(1)′−Eu−Se(4)′	83.75(4)
Se(2)−Eu−Se(4)′	153.88(3)	N(3)−Eu−Se(1)	74.51(14)
N(1)−Eu−Se(1)	136.2(2)	N(2)−Eu−Se(1)	144.2(2)
Se(1)′−Eu−Se(1)	60.84(3)	Se(2)−Eu−Se(1)	79.73(4)
Se(4)′−Eu−Se(1)	80.45(4)	C(1)−Se(1)−Hg	114.5(2)
C(1)−Se(1)−Eu′	115.4(2)	Hg−Se(1)−Eu′	87.23(4)
C(1)−Se(1)−Eu	121.0(2)	Hg−Se(1)−Eu	89.12(4)
Eu′−Se(1)−Eu	119.15(3)	C(7)−Se(2)−Hg	108.4(2)
C(7)−Se(2)−Eu	113.0(2)	Hg−Se(2)−Eu	92.14(4)
C(13)−Se(3)−Hg	101.4(2)	C(19)−Se(4)−Hg	108.1(3)
C(19)−Se(4)−Eu′	110.6(2)	Hg−Se(4)−Eu′	88.51(4)

[a] Symmetry transformations used to generate equivalent atoms: (′) $-x, -y, -z + 1$.

(**2**) All C and O atoms were restrained with esd 0.01 so that their U_{ij} components approximated isotropic behavior; all C or O atoms closer than 1.7 Å to each other were restrained with esd of 0.02 to have the same U_{ij} components; all atom−atom distances in the THF groups containing O(6) and O(7) were restrained to idealized values (Cambridge Structural Database).

(**3**) All C and O atoms were restrained with esd 0.02 so that their U_{ij} components approximated isotropic behavior; all C, Zn, or Se atoms closer than 1.7 Å to each other were restrained with an esd of 0.02 to have the same U_{ij} components; all atom−atom distances in the THF groups were restrained to idealized values; all phenyl rings were constrained to idealized hexagons.

(**4**) All Yb, Hg, and Se atoms were restrained with esd 0.02 so that their U_{ij} components approximated isotropic behavior; all atom−atom distances in all THF groups and the 1−2 and 1−3 Yb−THF and Se−phenyl distances were restrained to idealized values; all phenyl rings were constrained to idealized hexagons; all C atoms had fixed isotropic displacement parameters.

(**5**) All C and N atoms were restrained with esd 0.02 so that their U_{ij} components approximated isotropic behavior.

Results and Discussion

This paper illustrates how neutral donor, group 12 metal, and Ln/group 12 ratios can be systematically varied to give heterobi-, tetra-, penta-, and hexametallic benzeneselenolate compounds. The synthesis, structure, and UV−visible spectroscopic properties of the compounds are described, and the variety of structures are discussed in terms of the bonding character of the component metal ions.

Synthesis and Structure. Neutral Donor Ligand as a Variable: $[(py)_3Eu(\mu_2\text{-SePh})_2(\mu_3\text{-SePh})HgSePh]_2$ (1). Heterometallic selenolates can be isolated from donor solvents as basic as pyridine. In the first report describing lanthanide−group 12 metal selenolates, the visible spectrum of $[(THF)_3EuHg(SePh)_4]_2$ did not show the Eu(II) to pyridine charge transfer absorption characteristic of $Eu(SePh)_2$, and this was an indication that some

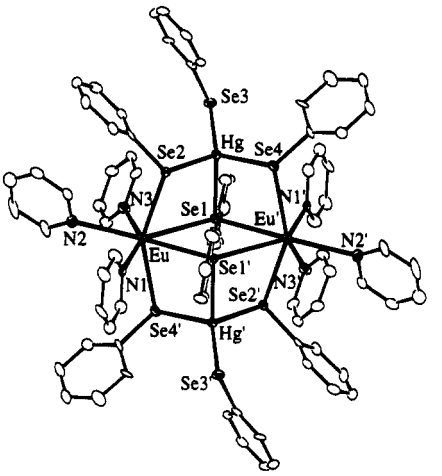

Figure 1. Molecular structure of $[(pyridine)_3Eu(\mu_2\text{-SePh})_2(\mu_3\text{-SePh})HgSePh]_2$ (**1**). The tetrametallic cluster contains seven-coordinate Eu(II) ions and tetrahedral Hg(II) ions connected through doubly and triply bridging selenolate ligands. From the Eu−pyridine charge transfer absorption energy, it is clear that the group 12 metal is withdrawing selenolate electron density away from the Eu ion and weakening the Eu−Se bond. Significant bond lengths (Å): Eu−μ_2−Se(2), 3.146(1); Eu−μ_2−Se(4), 3.153(1); Eu−μ_3−Se(1), 3.184(1); Hg−Se(3)(terminal), 2.545(1); Hg−μ_2−Se(2), 2.665(1); Hg−μ_2−Se(4), 2.688(1); Hg−μ_3−Se(1), 2.787(1); Eu−N (average), 2.67(1).

form of heterometallic structure was maintained in pyridine.[8] Since the persistence of heterometallic structure in a donor solvent as basic as pyridine would be an indication of the strength of the bimetallic stabilization, we sought to establish whether heterometallic complexes could be isolated as pyridine adducts. The room temperature reduction of Ph_2Se_2 with Eu/Hg gives $[(pyridine)_3Eu(\mu_2\text{-SePh})_2(\mu_3\text{-SePh})HgSePh]_2$ (**1**) in 90% yield. Low temperature single crystal X-ray diffraction showed that **1** is a tetrametallic cluster **1** containing pairs of seven-coordinate Eu(II) and tetrahedral Hg(II) ions connected by two μ_3 and four μ_2 benzeneselenolate ligands (Figure 1). The Eu coordination sphere is saturated with three neutral pyridine donors, and the Hg is bound to a terminal benzeneselenolate ligand. This cluster framework is identical to the recently reported THF derivative, and is structurally related to a number of tetrametallic mercury thiolates.[12] Table 2 gives a listing of significant bond geometries for **1**.

A comparison of Ln−Se bond lengths can be used to establish the effect of the group 12 metal on the Ln−Se bond. In both **1** and $[(THF)_2SmHg(SePh)_5]_2$, the Hg−Se bonds to the μ_3-Se are longer than those to the doubly bridging Se, while in $[(THF)_3EuHg(SePh)_4]_2$, there is little difference between Hg−μ_3-Se and Hg−μ_3-Se bond lengths. Similarly, if we look at the Ln−Se bonds, the difference between Ln−μ_2-Se and Ln−μ_3-Se bond lengths are 0.03 Å in **1**, 0.08 Å in $[(THF)_2SmHg(SePh)_5]_2$, and 0.13 Å in $[(THF)_3EuHg(SePh)_4]_2$. In all complexes, the soft, polarizable Hg−Se bonds are considerably more sensitive to local environments than the Ln−Se bonds. Comparison of the Eu−μ_2-Se bond lengths in the heterometallic compounds with the related Eu−Se bonds in the 1D coordination polymers[8] of $Eu(SePh)_2$ (3.14Å in $[(THF)_3Eu(\mu_2\text{-SePh})_2]_n$ and 3.10 Å in $[(py)_2Eu(\mu_2\text{-SePh})_2]_n$ shows virtually no effect in the THF complexes, while in the pyridine complexes, the Eu−N bonds in seven-coordinate **1** are, on average, 0.02 Å shorter than the Eu−N bonds in $[(py)_2Eu(\mu_2\text{-SePh})_2]_n$, while

(12) (a) Fawcett, T. G.; Ou, C.-C.; Potenza, J. A.; Schugar, H. J. *J. Am. Chem. Soc.* **1978**, *100*, 2058−62. (b) Canty, A. J.; Raston, C. L.; White, A. H. *Aust. J. Chem.* **1978**, *31*, 677. (c) Hu, W. J.; Barton, D.; Lippard, S. J. *J. Am. Chem. Soc.* **1973**, *95*, 1170−73.

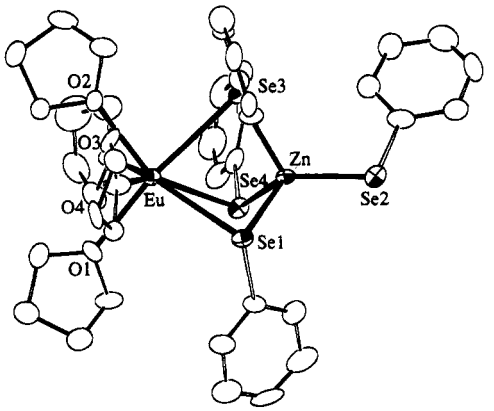

Figure 2. Molecular structure of the $(THF)_4Eu(\mu_3\text{-}SePh)_3Zn(SePh)$ (**2**). The more electronegative zinc(II) ion strongly polarizes chalcogen electron density away from the Eu(II) ion and so the resultant heterometallic structure contains only three Ln–Se bonds, rather than the four Ln–Se bonds found in **1**. There are two bimetallic molecules in the unit cell with nearly identical bond geometries. Significant bond lengths (Å): Eu(1)–Se(3), 3.162(2); Eu(1)–Se(4), 3.176(2); Eu(1)–Se(1), 3.282(2); Zn(1)–Se(2), 2.372(4); Zn(1)–Se(3), 2.514(3); Zn-(1)–Se(1), 2.514(3); Zn(1)–Se(4), 2.519(3); Zn–Se(2), 2.372(4); Eu–O (average), 2.54(1).

the Eu–Se bonds are 0.05 Å longer. In the pyridine complexes, these changes are interpreted in terms of the Hg^{2+} ion polarizing chalcogen electron density away from the lanthanide, thus slightly weakening the Eu–Se bonds and increasing the electrostatic attraction between the metal and the nitrogen donor.

Group 12 Metal as a Variable: $(THF)_4Eu(\mu_2\text{-}SePh)_3ZnSePh$ (2). Substitution of Zn for Hg illustrates how heterometallic chalcogenolate chemistry is general for the group 12 metals, and is important because heterometallic Ln–Zn complexes are interesting models for Ln ions doped into a ZnE matrix.[6j-l] The transmetalation reaction of $[(THF)_3EuHg(SePh)_4]_2$ with elemental Zn in THF proceeds rapidly at room temperature, depositing elemental Hg that can be identified visually. Crystallization from THF gives 80% yields of a heterometallic benzeneselenolate complex, and low temperature single crystal X-ray diffraction indicated showed that $(THF)_4Eu(\mu_2\text{-}SePh)_3ZnSePh$ (**2**) had been isolated. Figure 2 shows an ORTEP diagram of **2**, and Table 3 gives a listing of significant bond geometries for **2**.

Complex **2** is the first example of a bimetallic Ln–M chalcogenolate complex. In the structure, the tetrahedral Zn is bound to one terminal benzeneselenolate ligand, and the remaining three selenolates bridge the Eu and Zn ions. The Eu coordination sphere is saturated with four THF ligands. The structure of bimetallic **2**, rather than a tetrametallic cluster, can be rationalized in terms of significantly weakened Eu–Se bonds. In **2**, the Eu–Se bond lengths are 0.11Å longer than the Eu–Se distances found in the $Eu(SePh)_2$ coordination polymers. This lengthening is significantly greater than that found in the Hg derivatives because Zn forms stronger bonds to the chalcogen, thus competing more effectively for Se electron density. In **2**, this bond weakening is so strong that the final molecular structure contains three Eu–Se bonds, rather than the four Ln–Se bonds in the tetrametallic clusters.

Lanthanide–Group 2 Metal Ratio as a Variable: $[Sm(THF)_7][Zn_4(\mu_2\text{-}SePh)_6(SePh)_4]$ (3) and $[Yb(THF)_6][Hg_5(\mu_2\text{-}SePh)_8(SePh)_4]\cdot 2THF$ (4). Lanthanide benzeneselenolate bonds are cleaved in the presence of more than 1 equiv of $M(SePh)_2$. In an attempt to substitute Zn for Hg in the Sm(III) complex $[(py)_2SmHg(SePh)_5]_2$ using an excess of Zn, substitution of Hg was followed by reduction of the Sm(III) ion and the formation of $^1/_2$ equiv of $Zn(SePh)_2$. Eventually, purple needles precipitated from the reaction in 70% yield, and these needles were characterized by low temperature single crystal X-ray diffraction and shown to be $[Sm(THF)_7][Zn_4(\mu_2\text{-}SePh)_6(SePh)_4]$ (**3**). Table 4 gives a listing of significant bond geometries for **3**, and Figure 3 gives an ORTEP diagram of the $Sm(THF)_7$ dication, a rare example of a Ln ion coordinated only to weak neutral donors.[15] The adamantanoid dianion cluster $Zn_4(SePh)_{10}$ has considerable structural precedence in Group 2 metal chalcogenolate chemistry.[13,16] The Sm–O bond lengths (range: 2.51 to 2.58 Å) are consistent with a Sm(II) oxidation state.

Compound **3** represents an extreme example of how group 12 metals weaken lanthanide chalcogen bonds, as discussed for the structures of **1** and **2**. Reduction of Sm(III) by excess Zn

Table 3. Significant Bond Lengths (Å) and Angles (deg) for **2**

Eu(1)–O(2)	2.507(12)	Eu(1)–O(1)	2.537(12)
Eu(1)–O(4)	2.554(11)	Eu(1)–O(3)	2.559(12)
Eu(1)–Se(3)	3.162(2)	Eu(1)–Se(4)	3.176(2)
Eu(1)–Se(1)	3.282(2)	Eu(1)–Zn(1)	3.547(3)
Zn(1)–Se(2)	2.372(4)	Zn(1)–Se(3)	2.514(3)
Zn(1)–Se(1)	2.514(3)	Zn(1)–Se(4)	2.519(3)
Se(1)–C(1)	1.95(2)	Se(2)–C(7)	1.93(2)
Se(3)–C(13)	1.88(2)	Se(4)–C(19)	1.91(2)
O(2)–Eu(1)–O(1)	105.8(4)	O(2)–Eu(1)–O(4)	74.4(4)
O(1)–Eu(1)–O(4)	79.3(4)	O(2)–Eu(1)–O(3)	73.6(4)
O(1)–Eu(1)–O(3)	78.9(4)	O(4)–Eu(1)–O(3)	134.2(5)
O(2)–Eu(1)–Se(3)	82.8(3)	O(1)–Eu(1)–Se(3)	170.8(3)
O(4)–Eu(1)–Se(3)	100.3(3)	O(3)–Eu(1)–Se(3)	107.2(3)
O(2)–Eu(1)–Se(4)	136.2(3)	O(1)–Eu(1)–Se(4)	100.0(3)
O(4)–Eu(1)–Se(4)	146.1(3)	O(3)–Eu(1)–Se(4)	77.5(3)
Se(3)–Eu(1)–Se(4)	75.13(6)	O(2)–Eu(1)–Se(1)	140.4(3)
O(1)–Eu(1)–Se(1)	96.0(3)	O(4)–Eu(1)–Se(1)	77.9(3)
O(3)–Eu(1)–Se(1)	144.2(3)	Se(3)–Eu(1)–Se(1)	74.99(6)
Se(4)–Eu(1)–Se(1)	68.42(6)	O(2)–Eu(1)–Zn(1)	126.3(3)
O(1)–Eu(1)–Zn(1)	127.9(3)	O(4)–Eu(1)–Zn(1)	110.8(3)
O(3)–Eu(1)–Zn(1)	114.4(3)	Se(3)–Eu(1)–Zn(1)	43.53(5)
Se(4)–Eu(1)–Zn(1)	43.57(5)	Se(1)–Eu(1)–Zn(1)	42.97(5)
Se(2)–Zn(1)–Se(3)	118.71(11)	Se(2)–Zn(1)–Se(1)	113.08(11)
Se(3)–Zn(1)–Se(1)	102.62(10)	Se(2)–Zn(1)–Se(4)	124.87(12)
Se(3)–Zn(1)–Se(4)	100.32(10)	Se(1)–Zn(1)–Se(4)	92.39(10)
Se(2)–Zn(1)–Eu(1)	174.27(10)	Se(3)–Zn(1)–Eu(1)	60.05(7)
Se(1)–Zn(1)–Eu(1)	62.88(7)	Se(4)–Zn(1)–Eu(1)	60.35(7)

Table 4. Significant Bond Lengths (Å) and Angles (deg) for the Cation in **3**

Sm–O(3)	2.51(2)	Sm–O(1)	2.56(1)
Sm–O(5)	2.55(2)	Sm–O(4)	2.55(2)
Sm–O(2)	2.56(2)	Sm–O(7)	2.58(2)
Sm–O(6)	2.55(2)		
O(3)–Sm–O(6)	90.4(7)	O(3)–Sm–O(4)	84.7(8)
O(6)–Sm–O(4)	72.5(6)	O(3)–Sm–O(5)	81.0(7)
O(6)–Sm–O(5)	149.0(6)	O(4)–Sm–O(5)	77.0(6)
O(3)–Sm–O(1)	115.3(6)	O(6)–Sm–O(1)	134.7(6)
O(4)–Sm–O(1)	142.0(7)	O(5)–Sm–O(1)	75.0(6)
O(3)–Sm–O(7)	166.6(7)	O(6)–Sm–O(7)	76.7(8)
O(4)–Sm–O(7)	87.9(9)	O(5)–Sm–O(7)	108.2(8)
O(1)–Sm–O(7)	77.2(7)	O(3)–Sm–O(2)	77.9(7)
O(6)–Sm–O(2)	75.6(6)	O(4)–Sm–O(2)	143.4(7)
O(5)–Sm–O(2)	130.3(6)	O(1)–Sm–O(2)	74.5(6)
O(7)–Sm–O(2)	102.0(8)		

(13) Hagen, K. S.; Stephan, D. W.; Holm, R. H. *Inorg. Chem.* **1982**, *21*, 3928–36.
(14) *Inorg. Chem.*, in press.
(15) White, J. P.; Deng, H.; Boyd, E. P.; Gallucci, J.; Shore, S. G. *Inorg. Chem.* **1994**, *33*, 1685–94.
(16) (a) Calabrese, J.; Dance, I. *J. Chem. Soc., Chem. Commun.* **1975**, 762–3. (b) Dance, I. G. *J. Am. Chem. Soc.* **1979**, *101*, 6264–73. (c) Dance, I. G. *Inorg. Chem.* **1981**, *20*, 2155–60. (d) Hencher, J. L.; Khan, M.; Said, F. F.; Tuck, D. G. *Inorg. Nucl. Chem. Lett.* **1981**, *17*, 287–90. (e) Coucouvanis, D.; Kanatzidas, M.; Simhon, E.; Baenziger, N. C. *J. Am. Chem. Soc.* **1982**, *104*, 1874–82. (f) Hagen, K. S.; Holm, R. H. *Inorg. Chem.* **1983**, *22*, 3171–4. (g) Hagen, K. S.; Holm, R. H. *Inorg. Chem.* **1984**, *23*, 418–27.

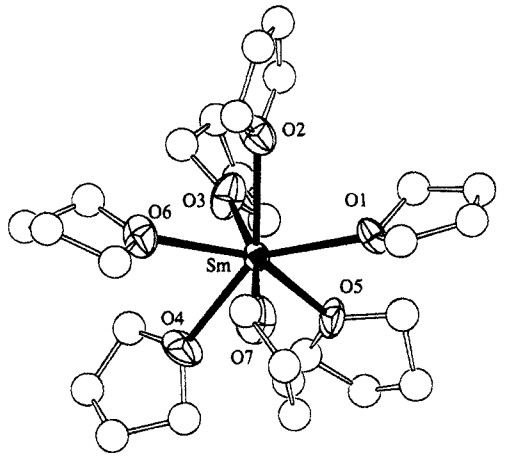

Figure 3. Molecular structure of cation in $[Sm(THF)_7]^{2+}[Zn_4(\mu_2\text{-}SePh)_6(SePh)_4]^{2-}$ (**3**). The reaction of $[(THF)_2SmHg(SePh)_5]_2$ with excess Zn leads to substitution of the Hg, reduction of the Sm(III) to Sm(II), and eventual precipitation of this purple cation/anion pair. The compound, which is a rare example of a lanthanide ion coordinated only to weak donor ligands, represents the extreme example of how group 12 metal chalcogenolates influence lanthanide−chalcogenolate bonds. The tetrametallic adamantanoid dianion structure has precedent in the literature. Average bond lengths (Å): Zn−μ_2-Se, 2.49(2); terminal Zn−Se, 2.41(1); Sm−O, 2.55(1).

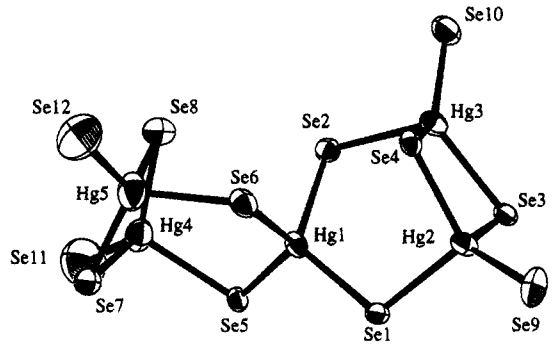

Figure 4. Molecular structure of the pentametallic dianion in **4**. Compound **4** is unstable in donor solvents other than THF. When **4** is dissolved in CH_3CN, $Hg(SePh)_2$ precipitates, and when **4** is dissolved in pyridine, elemental Hg precipitates and a paramagnetic Yb(III) compound forms. Significant bond lengths (Å): Hg(1)−Se(6), 2.636(7); Hg(1)−Se(2), 2.641(6); Hg(1)−Se(5), 2.644(7); Hg(1)−Se(1), 2.674(7); Hg(2)−Se(9), 2.564(9); Hg(2)−Se(1), 2.696(7); Hg(2)−Se(4), 2.703(6) ; Hg(2)−Se(3), 2.715(6); Hg(3)−Se(10), 2.495(7); Hg(3)−Se(4), 2.707(6); Hg(3)−Se(3), 2.719(6); Hg(3)−Se(2), 2.726(7); Hg(4)−Se(11), 2.50(2); Hg(4)−Se(8), 2.688(10); Hg(4)−Se(5), 2.726(6); Hg(4)−Se(7), 2.765(7); Hg(5)−Se(12), 2.546(11); Hg(5)−Se(7), 2.637(8); Hg(5)−Se(6), 2.675(8); Hg(5)−Se(8), 2.867(11).

gives $^1/_2$ equiv of $Zn(SePh)_2$ in solution, and in the presence of this excess group 12 metal chalcogenolate, a more stable anion configuration, with selenolate anionic charge delocalized throughout the four Zn ions, can be constructed. The reduction of Sm(III) by Zn indicates how poorly chalcogenolate ligands stabilize trivalent lanthanides: in aqueous solution, Zn ($E° = -0.76$ eV) reduces Eu(III) ($E° = -0.43$ eV), but not Sm(III) ($E° = -1.55$ eV).

In order to probe the solution structures of these 1:4 Ln:M heterometallics using ^{1}H NMR spectroscopy, we began working with Yb(II), which has a diamagnetic (f^{14}) ground state. The reaction of Yb metal with 5 equiv of PhSeSePh, in the presence of excess mercury (in theory, to form $[Yb(THF)_6][Hg_4(SePh)_{10}]$) gave excellent yields of a yellow crystalline solid. Examination of the product by ^{1}H NMR spectroscopy suggested that the product contained an 8:12 THF:SePh ratio. Elemental analysis was uninformative because the compound was extremely

Table 5. Significant Bond Lengths (Å) and Angles (deg) for the Anion in **4**

Hg(1)-Se(6)	2.636(7)	Hg(4)-Se(11)	2.50(2)
Hg(2)-Se(9)	2.564(9)	Hg(4)-Se(7)	2.765(7)
Hg(2)-Se(3)	2.715(6)	Hg(5)-Se(6)	2.675(8)
Hg(3)-Se(2)	2.726(7)	Hg(1)-Se(1)	2.674(7)
Hg(4)-Se(5)	2.726(6)	Hg(2)-Se(4)	2.703(6)
Hg(5)-Se(7)	2.637(8)	Hg(3)-Se(3)	2.719(6)
Hg(1)-Se(2)	2.641(6)	Hg(4)-Se(8)	2.688(10)
Hg(2)-Se(1)	2.696(7)	Hg(5)-Se(12)	2.546(11)
Hg(3)-Se(10)	2.495(7)	Hg(5)-Se(8)	2.867(11)
Se(6)-Hg(1)-Se(5)	119.8(2)	Se(6)-Hg(1)-Se(2)	102.6(2)
Se(2)-Hg(1)-Se(5)	101.5(2)	Se(6)-Hg(1)-Se(1)	104.2(2)
Se(2)-Hg(1)-Se(1)	118.3(2)	Se(5)-Hg(1)-Se(1)	111.0(2)
Se(9)-Hg(2)-Se(1)	116.7(2)	Se(9)-Hg(2)-Se(4)	120.0(3)
Se(1)-Hg(2)-Se(4)	103.0(2)	Se(9)-Hg(2)-Se(3)	118.7(2)
Se(1)-Hg(2)-Se(3)	98.0(2)	Se(4)-Hg(2)-Se(3)	96.5(2)
Se(10)-Hg(3)-Se(4)	129.9(3)	Se(10)-Hg(3)-Se(3)	122.6(2)
Se(4)-Hg(3)-Se(3)	96.3(2)	Se(10)-Hg(3)-Se(2)	96.9(2)
Se(4)-Hg(3)-Se(2)	97.9(2)	Se(3)-Hg(3)-Se(2)	109.8(2)
Se(11)-Hg(4)-Se(8)	130.3(4)	Se(11)-Hg(4)-Se(5)	109.5(4)
Se(8)-Hg(4)-Se(5)	108.7(3)	Se(11)-Hg(4)-Se(7)	110.9(4)
Se(8)-Hg(4)-Se(7)	94.7(3)	Se(5)-Hg(4)-Se(7)	97.0(2)
Se(12)-Hg(5)-Se(7)	123.5(4)	Se(12)-Hg(5)-Se(6)	110.7(4)
Se(7)-Hg(5)-Se(6)	113.6(2)	Se(12)-Hg(5)-Se(8)	118.7(4)
Se(7)-Hg(5)-Se(8)	93.4(3)	Se(6)-Hg(5)-Se(8)	91.3(3)
C(11)-Se(1)-Hg(1)	101.7(13)	C(11)-Se(1)-Hg(2)	96.8(8)
Hg(1)-Se(1)-Hg(2)	107.4(2)	C(21)-Se(2)-Hg(1)	102.1(5)
C(21)-Se(2)-Hg(3)	106.5(12)	Hg(1)-Se(2)-Hg(3)	105.3(2)
C(31)-Se(3)-Hg(2)	102.3(5)	C(31)-Se(3)-Hg(3)	100.1(8)
Hg(2)-Se(3)-Hg(3)	82.3(2)	C(41)-Se(4)-Hg(2)	102.2(9)
C(41)-Se(4)-Hg(3)	99.8(6)	Hg(2)-Se(4)-Hg(3)	82.8(2)
C(51)-Se(5)-Hg(1)	102.8(12)	C(51)-Se(5)-Hg(4)	94.8(5)
Hg(1)-Se(5)-Hg(4)	102.3(2)	C(61)-Se(6)-Hg(1)	101.5(6)
C(61)-Se(6)-Hg(5)	106.3(12)	Hg(1)-Se(6)-Hg(5)	108.6(3)
C(71)-Se(7)-Hg(5)	107.3(10)	C(71)-Se(7)-Hg(4)	92.2(4)
Hg(5)-Se(7)-Hg(4)	85.7(2)	C(81)-Se(8)-Hg(4)	99.9(9)
C(81)-Se(8)-Hg(5)	96.0(8)	Hg(4)-Se(8)-Hg(5)	82.8(2)

sensitive to desolvation, and so the compound was examined by low temperature single crystal X-ray diffraction and shown to be $[Yb(THF)_6][Hg_5(SePh)_{12}]\cdot 2THF$ (**4**), a separated cation/anion pair with a pentametallic dianion cluster. Table 5 gives a listing of significant bond geometries for **4**, and Figure 4 shows an ORTEP diagram of the pentametallic dianion. The octahedral lanthanide ion coordination sphere is composed entirely of neutral donor atoms, as found for **3**, with the difference in lanthanide coordination numbers being attributed to the smaller size of the Yb ion. The Yb−O bond length average (2.53(2) Å) is consistent with a divalent Yb ion. The mercury geometries are all distorted tetrahedra.

The $Hg_5(SePh)_{12}$ dianion appears to have no precedence in group 12 metal chalcogenolate chemistry, but experiments suggest that the potential energy surface defining the stability of this anion is shallow, and that alternative solution structures are readily accessible. As found for **1** and **2**, an NMR analysis of **4** in THF shows that there is only one type of benzeneselenolate resonance, indicating that bridging and terminal selenolates, if they are both present in THF, are exchanging rapidly on an NMR time scale. Rapid chalcogenolate site exchange processes have precedent in the literature.[13]

The stability of **4** depends significantly on the identity of the solvent. When **4** was dissolved in acetonitrile, crystalline $Hg(SePh)_2$ slowly precipitated from solution. The precipitation is not quantitative, and while the final heterometallic product has not been identified, roughly 10% of the initial $Hg(SePh)_2$ was isolated after a period of days. This observation can be explained by noting the nonstatic structure of these complexes and the insolubility of $Hg(SePh)_2$ in acetonitrile.

Not only is the ratio of M:Ln solvent dependent but in addition the oxidation state of the lanthanide ion can be

Table 6. Significant Bond Lengths (Å) and Angles (deg) for **5**[a]

Sm–N(1)	2.536(9)	Se(3)–Na	2.856(5)
Sm–Se(3)	2.977(2)	Na–Se(2)	2.835(5)
Sm–Se(4)	3.048(1)	Sm–Se(1)	2.908(1)
Na–N(4)	2.50(1)	Sm–Se(5)	2.990(1)
Sm–N(2)	2.551(8)	Na–N(3)	2.46(1)
Sm–Se(2)	2.980(1)		
N(1)–Sm–N(2)	155.7(3)	N(1)–Sm–Se(1)	82.7(2)
N(2)–Sm–Se(1)	73.8(2)	N(1)–Sm–Se(3)	95.7(2)
N(2)–Sm–Se(3)	92.6(2)	Se(1)–Sm–Se(3)	95.48(4)
N(1)–Sm–Se(2)	89.5(2)	N(2)–Sm–Se(2)	86.3(2)
Se(1)–Sm–Se(2)	94.45(4)	Se(3)–Sm–Se(2)	169.27(4)
N(1)–Sm–Se(5)	73.6(2)	N(2)–Sm–Se(5)	130.7(2)
Se(1)–Sm–Se(5)	152.86(4)	Se(3)–Sm–Se(5)	74.38(3)
Se(2)–Sm–Se(5)	98.32(3)	N(1)–Sm–Se(4)	127.3(2)
N(2)–Sm–Se(4)	74.6(2)	Se(1)–Sm–Se(4)	147.32(4)
Se(3)–Sm–Se(4)	93.99(3)	Se(2)–Sm–Se(4)	75.42(3)
Se(5)–Sm–Se(4)	59.67(4)	Na′–Se(2)–Sm	106.2(1)
Na–Se(3)–Sm	109.4(1)	N(3)–Na–N(4)	122.5(4)
N(3)–Na–Se(2)′	102.6(3)	N(4)–Na–Se(2)′	98.3(3)
N(3)–Na–Se(3)	98.5(3)	N(4)–Na–Se(3)	105.6(3)
Se(2)′–Na–Se(3)	132.1(2)		

[a] Symmetry transformations used to generate equivalent atoms: (′) $-x+1, y, -z+3/2$.

influenced by solvent donor strength. When yellow **4** was dissolved in pyridine, a deep red solution color developed instantly, and within seconds elemental mercury precipitated from the pyridine solution. From NMR spectroscopic analysis we can conclude that the ytterbium containing reaction product is paramagnetic, as judged by the 13–97 Hz line widths in the ^{1}H NMR spectrum. Again, the selenolate ligands are exchanging rapidly, and there is only one broadened set of benzeneselenolate resonances in the NMR spectrum. This redox behavior is consistent with the hard Lewis acid character of the lanthanides—addition of the stronger pyridine donor favors oxidation of Yb(II) to Yb(III) and concomitant reduction of Hg(II) to elemental Hg(0).

Clearly, this bimetallic theme is extremely general. Donor ligands, Ln oxidation state, group 12 metals, and ratios of Ln:M are all possible variables, and other work in our laboratory indicates that the chalcogen is yet another permutable component.[14] The stability gained upon coordination of highly unstable lanthanide-bound benzeneselenolates to the softer metal ion is the driving force in the reaction. This is reflected in the molecular structures of **1**–**4**, which have terminal group 12 selenolate ligands but no terminal lanthanide selenolate ligands. This coordination is entirely consistent with the well-documented stability of group 12 chalcogenolate complexes and the extreme air sensitivity of the lanthanide chalcogenolates.

Heterometallic Lanthanide–Alkali Metal Chalcogenolates: $[(py)_2Sm(SePh)(\mu\text{-}SePh)_3Na(py)_2]_2$ (5). The structural characterization of tetrametallic $[(py)_2Sm(SePh)(\mu\text{-}SePh)_3Na(py)_2]_2$ (**5**) afforded a unique opportunity to establish how substitution of an ionic metal for the group 12 metal influences tetrametallic cluster structure. Table 6 gives a listing of significant bond geometries for **5**, and Figure 5 gives an ORTEP diagram of **5**. This heterometallic chalcogenolate cluster, which crystallizes from the salt elimination reaction of $SmCl_3$ with NaSePh, contains two seven-coordinate Sm(III) ions and two tetrahedral Na ions, all connected by μ_2-SePh ligands. The Sm ion has a terminal benzeneselenolate ligand, and the Sm coordination sphere is saturated with two pyridine donors. The Na ions are also bound to two pyridine ligands. The electropositive nature of the component metals in **5** result in a structure having fewer M–Se bonds and more bonds between metals and neutral donor ligands, as found in **2**, and in contrast to the tetrametallic structures of **1**, $[(THF)_3EuHg(SePh)_4]_2$, and

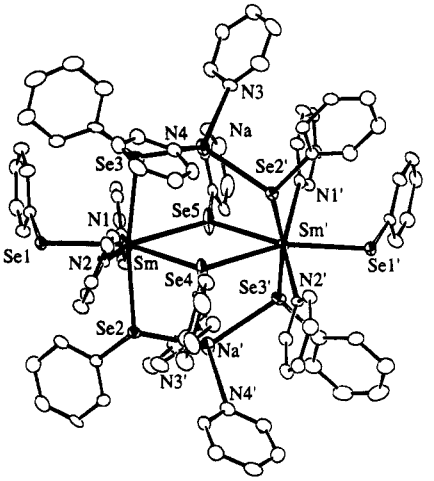

Figure 5. Molecular structure of $[(py)_2Sm(SePh)(\mu\text{-}SePh)_3Na(py)_2]_2$ (**5**). The tetrametallic cluster framework is present in **5**, but replacement of the group 12 metals by less chalcophilic Na ions results in a structure with fewer bridging selenolate interactions and an increase in the number of hard donor ligands coordinated to the cluster. Significant bond lengths (Å): Sm–Se(1), 2.908(1); Sm–Se(3), 2.977(2); Sm–Se(2), 2.980(1); Sm–Se(5), 2.990(1); Sm–Se(4), 3.048(1); Se(3)–Na, 2.856(5); Na–Se(2), 2.835(5); Sm–N(average), 2.54(1); Na–N, 2.48(2).

$[(THF)_2SmHg(SePh)_5]_2$.[14] Examination of the Sm–Se bonds in **5** with the Sm–Se bonds in $[(THF)_2SmHg(SePh)_5]_2$ indicates that the soft Hg(II) ion does not significantly perturb the Sm(III)–Se bond length.

Characterization by UV–Visible Spectroscopy. UV–visible spectroscopic characterization of these heterometallic molecules indicates that the group 12 metal polarizes selenolate electron density away from the lanthanide ion. This effect is observed in both Ln(II) and Ln(III) compounds. The intense (ϵ_o ca. 4×10^4 M^{-1} cm^{-1}) broad visible absorptions of $Ln(EPh)_2(py)_x$ (Ln = Eu, Yb) complexes have been assigned as metal-to-pyridine charge transfer excitations.[5f] This assignment is based on the absence of an absorption in the related THF complexes and the fact that in isostructural $Ln(TePh)_2(py)_5$, the absorption of the Eu complex is ca. 0.9 eV greater than that of the Yb compound. In pyridine, divalent **1** has a metal to pyridine charge transfer absorption (λ_{max} = 380 nm), which, when compared with the corresponding absorption for $Eu(SePh)_2$ in pyridine (λ_{max} = 392 nm),[5d] indicates that it is more difficult to oxidize the Eu(II) ion in **1**. Replacement of Hg by Zn in **2** further increases the MLCT energy, with the visible spectrum of **2** in pyridine showing an absorption maximum at 352 nm. The UV–visible data are consistent with longer Eu–Se bonds in **2**, as well as fewer Eu–Se bonds in **2** relative to **1** or the $Eu(SePh)_2$ coordination polymers. Both physical measurements indicate that the group 12 metal polarizes Se electron density away from the Ln ion.

The colors of the Sm(III) heterometallic chalcogenolates are also consistent with the group 2 metal ion withdrawing electron density from the lanthanide ion. The visible spectra of certain Ln(III) chalcogenolates are dominated by intense chalcogen to metal charge transfer absorptions that were assigned from a comparison of the visible spectra of $[(py)_3Ln(SePh)_3]_2$ (Ln = Ho, Tm, Yb).[5m] The Na–Sm complex **5** is light yellow in solution and in crystalline form, and any Se-to-Sm charge transfer excitation must be found in the UV spectrum. In contrast, $[(THF)_2SmHg(SePh)_5]_2$ is deep red.[8] There is no discrete absorption maximum in the visible spectrum of the Sm–Hg complex, but the fact that the CT absorption has shifted from UV to visible radiation suggests the Hg ion is polarizing

Se electron density away from the Sm(III) ion and lowering the energy required to reduce the Sm(III).

Conclusion

Heterometallic Ln−group 12 metal chalcogenolate complexes are an extremely broad class of molecules in which neutral donor, group 12 metal, Ln oxidation state, and the ratio of Ln:M are all potential variables. Because the hard, ionic Ln ions are stabilized only by soft, covalent benzeneselenolate and weak neutral donor ligands, the resultant complexes are relatively unstable, and the Ln−Se bond is readily distorted. The weakness of the Ln−Se bond leads to a variety of molecular heterometallic structures.

The tetrametallic Ln_2Hg_2 benzeneselenolate cluster is a recurring structural motif in which selenolate ligands bound to Ln ions are stabilized by coordination to a soft Hg(II) ion. Substitution of Hg with Zn increases the Ln−Se bond lengths, and results in the formation of a bimetallic structure containing fewer Ln−chalcogen bonds. An extreme example of this bond lengthening results when excess $M(SePh)_2$ (M = Hg, Zn) reacts with $Ln(SePh)_2$ to completely remove the SePh from the Ln coordination sphere. Even the identity of the neutral donor ligand can influence heterometallic structure: both the ratio of Ln:M and the Ln oxidation state are potentially solvent dependent.

Acknowledgment. This work was supported by the National Science Foundation under Grant No. CHE-9204160.

Supporting Information Available: Tables of crystallographic data and refinement results, atomic coordinates, additional bond lengths and angles, anisotropic displacement parameters, and hydrogen bond parameters and figures giving fully labeled ORTEP diagrams for **1**−**5** (49 pages). This material is contained in many libraries on microfiche, immediately follows this article in the microfilm version of the journal, and can be ordered from the ACS; see any current masthead page for ordering information. Structure factor tables are available from the authors.

IC950715G